Electronic supplementary information (ESI)

Precise determination of the nanoparticle concentration and ligand density of engineered water-soluble HgSe fluorescent nanoparticles

Diego Bouzas-Ramos, Mario Menéndez-Miranda, José M. Costa-Fernández, Jorge Ruiz Encinar* and Alfredo Sanz-Medel*

Supplementary tables

Table S1 ICP-MS settings and operating conditions.

Plasma parameters	RF Power	1550 W
	RF Matching	1.93 V
	Sample Depth	7.0 mm
	Carrier Gas (Ar)	0.90 L min^{-1}
	Makeup Gas (Ar)	0.25 L min^{-1}
Lenses	Extract 1	0.0 V
	Extract 2	-190.0 V
	Omega Bias	-110 V
	Omega Lens	10.2 V
	Deflect	-12.2 V
	Plate Bias	-60 V
Cell	O_2 Flow	0.35 mL min^{-1}
	Oct Bias	-18.0 V
	Oct RF	200 V
Transitions (Q1→Q2)	$Se^+ \rightarrow SeO^+$	Mass shift
	$Hg^+ \rightarrow Hg^+$	On mass
	$S^+ \rightarrow SO^+$	Mass shift

Table S2 AF4 separation conditions.

Injection time (min)	3
Injection volume (µL)	20
Transition time (min)	1
Tip flow rate (mL min^{-1})	0.2
Initial cross flow rate (mL min^{-1})	2.5
Cross flow linear decay (min)	25
Detector flow rate (mL min^{-1})	1
Carrier	2 g L^{-1} Ammonium acetate, 0.01% (w/v) SDS, pH 10
Separation membrane type	Polyether sulfone (PES), cutoff 10 kDa
Separation channel dimensions	27.5 cm length, 500 µm thickness

Supplementary figures

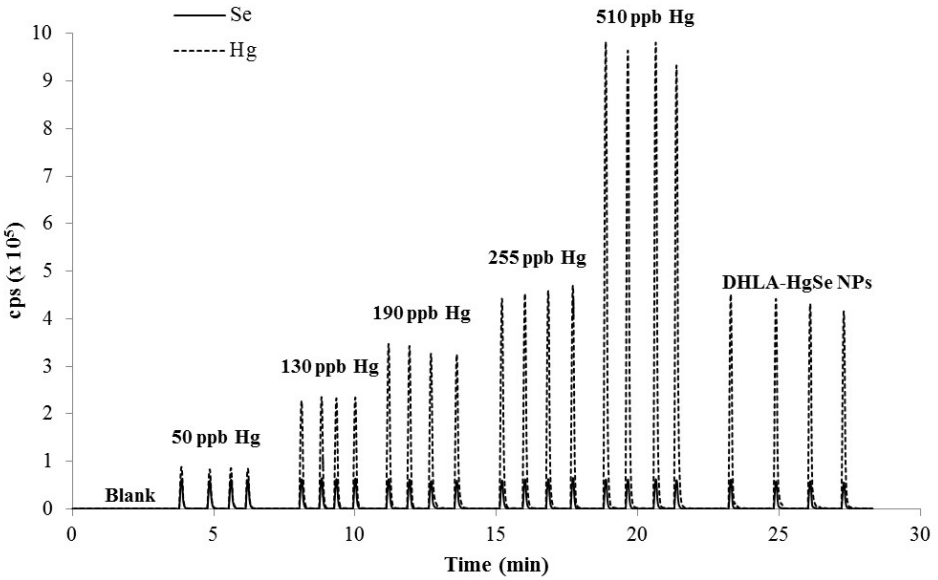

Fig. S1 Molar calibration plot built from FIA of mixtures of Se and Hg ICP standards. Selenium concentration kept constant at 100 ppb for every standard (Fig. S1). Several replicates were carried out for every individual point and the sample. Precision associated ranged 1 – 3% RSD.

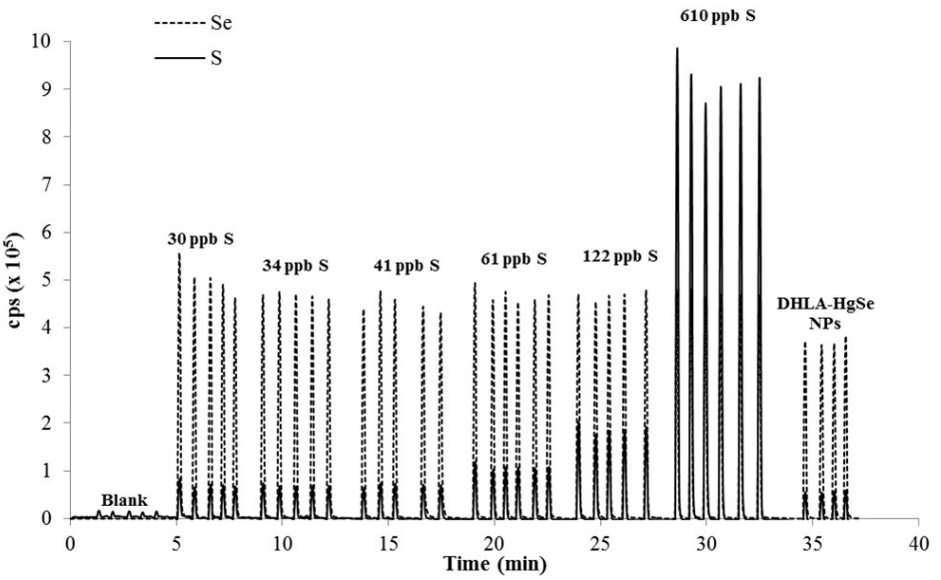

Fig. S2 Molar calibration plot built from FIA of mixtures of Se and S ICP standards. Selenium concentration kept constant at 1500 ppb for every standard (Fig. S2). Several replicates were carried out for every individual point and the sample. Precision associated ranged 1 – 3% RSD.

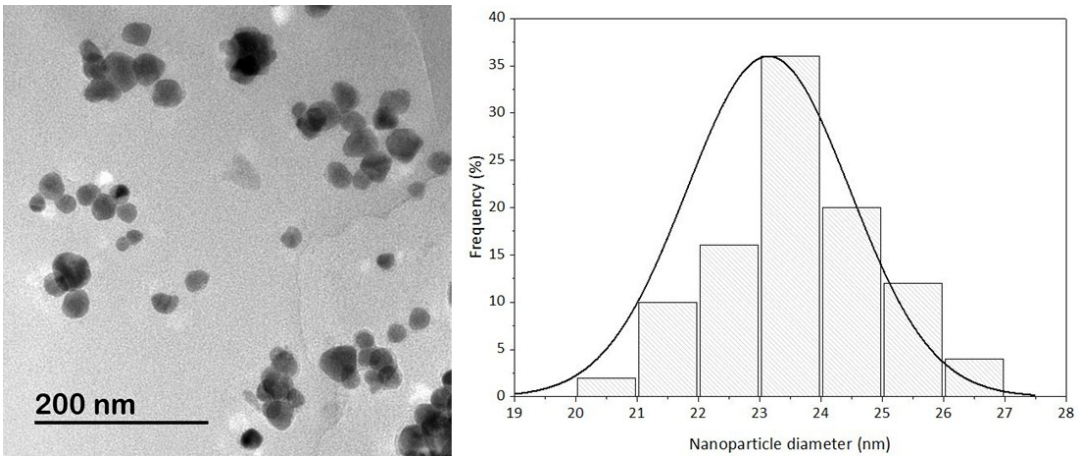

Fig. S3 HR-TEM image and nanoparticle size distribution histogram of the HgSe NPs. Nanoparticle sizes in Fig. S3 were measured by counting HR-TEM image by digital analysis employing the ImageJ software of image processing.

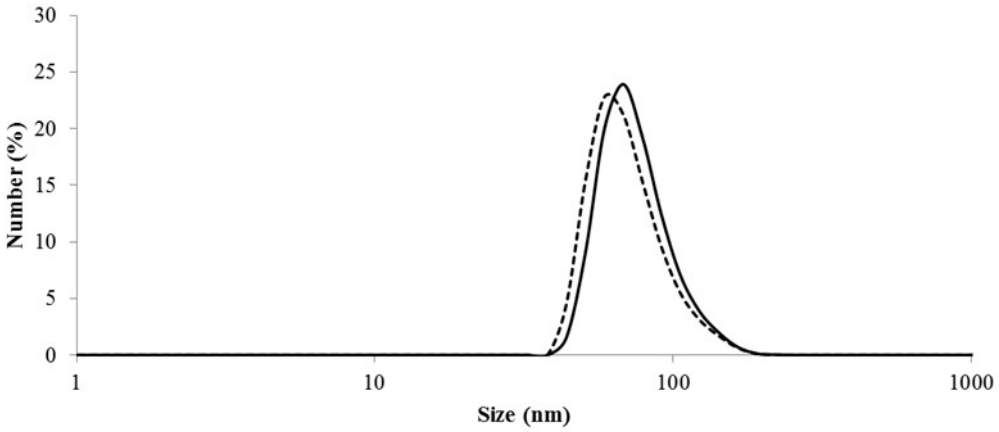

Fig. S4 DLS size distributions of the nanoparticle suspensions. Solid line: “DHLA-capped HgSe NPs”; Dashed line: “HgSe NPs”.

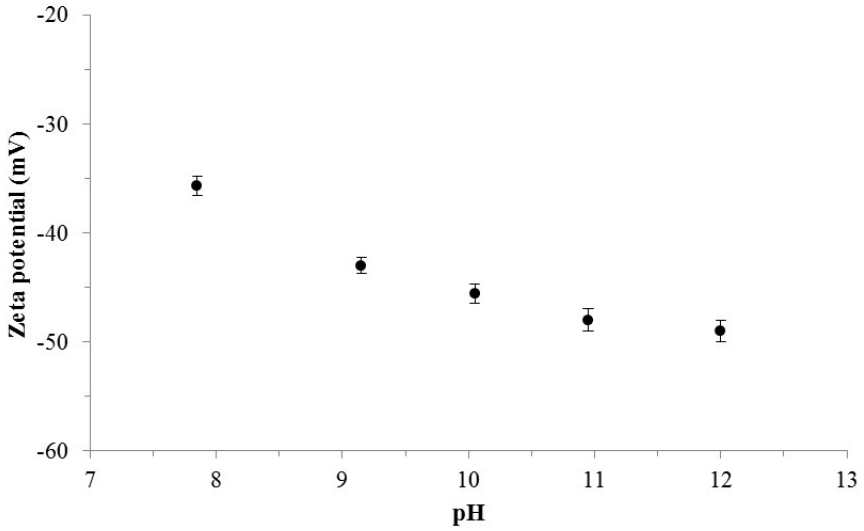

Fig. S5 Zeta potential measurements of the DHLA-capped HgSe NPs in water media as a function of pH. Precision associated ranged 1 – 2% RSD (*n*=6).

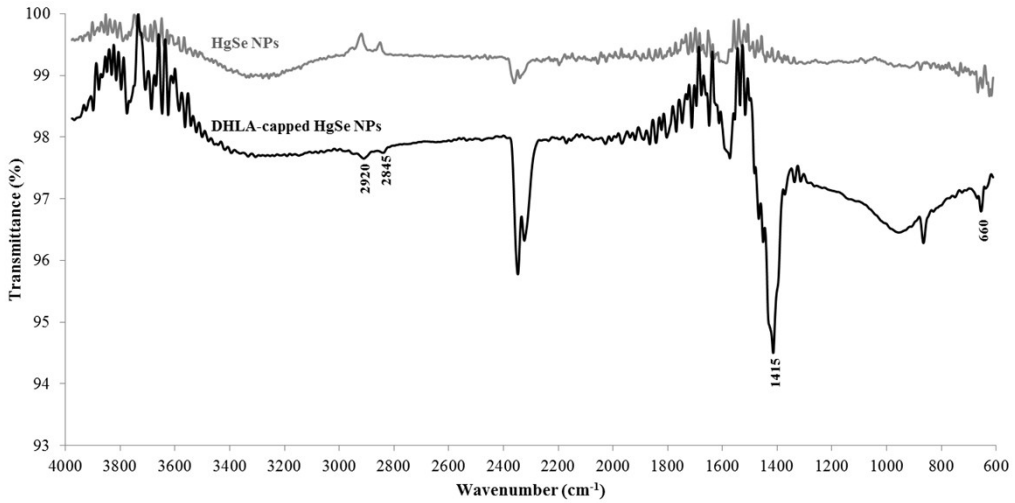

Fig. S6 FT-IR spectra of the HgSe NPs (line in grey) and DHLA-capped HgSe NPs (line in black). Spectral bands of residual atmospheric components are present in both spectra: the peak at 2335 cm^{-1} is corresponding to CO_2 and noisy regions at 3800 and 1600 cm^{-1} are attributed to H_2O.

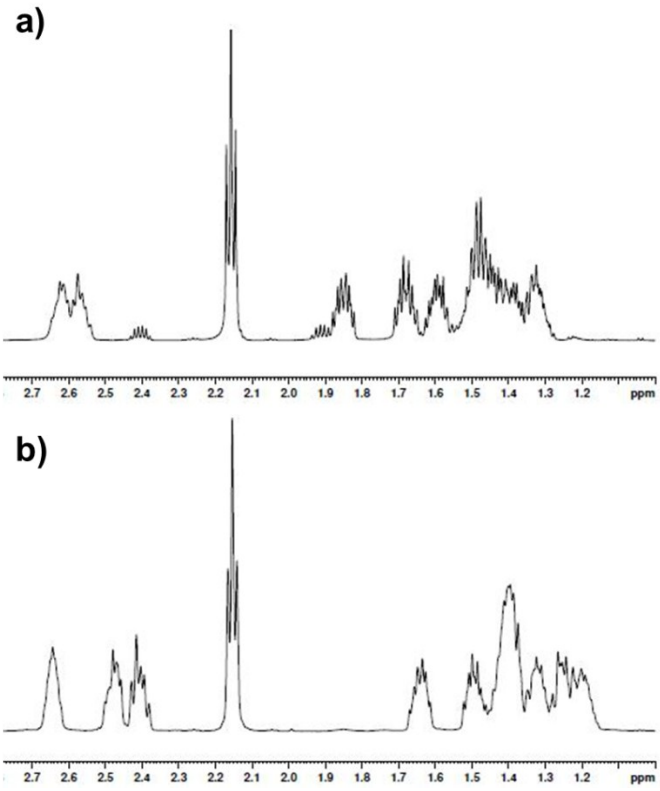

Fig. S7 ^{1}H-NMR spectra of the (a) DHLA-capped HgSe NPs, and (b) free DHLA. Both samples were prepared in deuterium oxide (D_2O) solution before the NMR measurements.

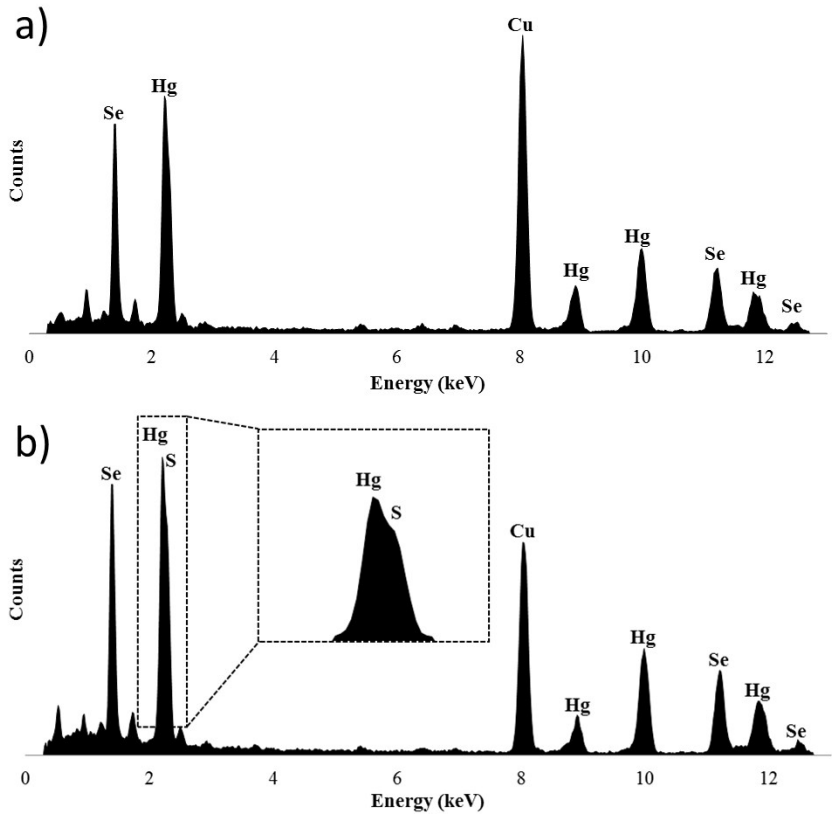

Fig. S8 EDX spectrum of the (a) HgSe NPs, and (b) HgSe NPs capped with DHLA. Only a Cu peak (Fig. S8), related to the copper grid used as sample holder, was detected as an impurity. Extended peak in Fig. S8b showed a shoulder that corresponds to detected sulphur in the DHLA-HgSe NPs.

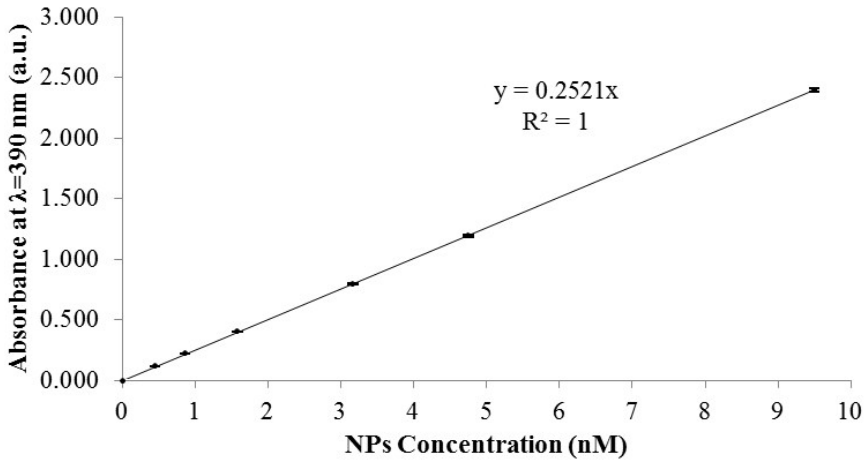

Fig. S9 Calibration curve of the absorbance values obtained versus the concentration (nM) of the DHLA-capped HgSe NPs solution. Uncertainty bars correspond to 1 SD (*n*=3).